Proton induced luminescence of minerals

H. Calvo del Castillo[a,b,d], A. Millán [a], P. Beneítez [c], J.L. Ruvalcaba-Sil [b], T. Calderón [a]

[a]*Depto. Geología y Geoquímica, Universidad Autónoma de Madrid, Ctra. Colmenar, km. 15, 28049, Madrid, Spain.*
[b]*Instituto de Física, Universidad Nacional Autónoma de México, Circuito de la Investigación Científica s/n,*
Ciudad Universitaria, México D.F. 04510, México.
[c]*Departamento Química Física Aplicada. Universidad Autónoma de Madrid Cantoblanco, Madrid, Spain.*
[d]*Centre Européen dArchéométrie – IPNAS, Université de Liège, Allée du 6 Août, BAT 15, 4000, Sart Tilman, Liège, Belgium.*

This paper presents a summary of Ionoluminescence (IL) for several minerals commonly found in jewellery pieces and/or artefacts of historical interest. Samples including silicates and non-silicates (native elements, halide, oxide, carbonate and phosphate groups) have been excited with a 1.8 MeV proton beam, and IL spectra in the range of 200- 900 nm have been collected for each one using a fiber optic coupled spectrometer. Light emissions have been related to Cr^{3+}, Mn^{2+} and Pr^{3+} ions, as well as intrinsic defects in these minerals. Results show the potential of IL for impurity characterization with high detection limits, local symmetry studies, and the study of the origin of minerals.

Keywords: Ionoluminescence; mineral; gemstone; light emission; defects; impurities.

En este trabajo se presenta un resumen sobre la Ionoluminiscencia (IL) de varios minerales de uso común en piezas y/o artefactos de joyería de interés histórico. Las muestras estudiadas incluyen minerales del grupo de los silicatos y no silicatos (elementos nativos, haluros, óxidos, carbonatos y fosfatos) y fueron excitadas con un haz de protones de 1,8 Mev, siendo el espectro de IL recogido en el rango de 200-900 nm usando una fibra óptica acoplada a un espectrómetro. Las emisiones de luz detectadas han sido relacionadas con la presencia diversos iones en estos minerales, tales como de Cr $^{3+}$, Mn $^{2+}$ y Pr $^{3+}$, así como a la presencia de defectos intrínsecos . Los resultados obtenidos muestran el potencial de IL para la caracterización de impurezas a bajo niveles de concentración, el estudio de simetrías locales y estudio de procedencia de minerales.

Descriptores: Ionoluminiscencia; mineral; emisión de luz; defectos; impurezas.

PACS: 78.60.Hk, 91.60.Ed, 61.72.Ss, 29.27.-a, 87.66.-a, 82.80.-d

1. Introduction

Despite the frequent application of other luminescent techniques to minerals in Earth Sciences, covering issues that go from impurities characterization [1-2] to mineral exploration [3] or quaternary age dating [4-6], Ionoluminescence (IL) still remains a relatively underdeveloped technique fi, however, to determining the chemical valence state of optical active impurities, present inside a mineral lattice, and thus, contributing to the unravelling of the general mechanisms of ion beam interaction with matter.

Recent applications of IL to minerals include the following: impurity characterization of inorganic solids and microanalysis of inclusions [7-8], damage caused on samples during proton irradiation for PIXE measurements [9], or studies on the relationship between emission wavelength and bonding distance inside mineral structures [10]. Recently Ionoluminescence has been also proposed as a tool for distinguishing imitation from natural diamonds [11].

Most of the minerals examined in this work have previously undergone other luminescent techniques [1-2,12-16], for it is fully believed that previous experience developed in impurity characterization is to be very useful to the understanding of IL, and will therefore contribute to the establishing of an IL data base.

This paper presents a rapid summary on IL for mineral cases usually found in jewellery and artefacts of historical interest, that emphasize the potential of the technique, in particular its ability to detect crystal defects and impurities at very low concentrations (less than a few $\mu g/g$).

2. Experimental

Twenty-one different mineral samples, including silicates and non-silicates, were selected for this study (Table I). All natural samples used were previously characterized by other luminescence methods, atomic absorption spectroscopy and X-ray diffraction [1-2,12-16].

IL measurements were carried out at the Pelletron Accelerator of the Instituto de Física (Universidad Nacional Autónoma de México). No sample preparation was required. A 1.8 MeV proton beam was impinged at 45° from the sample surface for excitation, inside a vacuum chamber. Current intensity varied from 150 nA to 2.8 μA as different species have different sensitivity towards the luminescent process. Light emitted was collected at 90° by means of two optic fibres connected by a vacuum feedthrough: an inside-chamber one, 1mm in diameter and 1 m length and supplied with an Ocean Optics 74UV lens, set at 2cm from the sample's surface; and an outside-chamber one, 600μm in diameter and 1 m in length, connected to the USB2000 Ocean Optics Spectrometer. The spectrometer has an entrance aperture of 25 μm wide by 1mm height and a grating corresponding to a spectral range from 200 to 900 nm. Thus, its optical resolution is 0.8 nm. Measurements were taken for just a few seconds for each sample and sample cooling was not carried out.

TABLE I. Mineral samples studied for this work.

Mineral	General Composition	Colours
Diamond	C	Yellow
		Brown
		Orange
		Milk-white
Fluorite	CaF_2	Green, Dark
		blue, light
		blue, pink
		and ultrapure
		synthetic
		colourless
Ruby	Al_2O_3	Red
Sapphire		Blue, Pink
Calcite	$CaCO_3$	Colourless
Strontianite	$SrCO_3$	Colourless
Apatite	$Ca_5(PO_4)_3(F,Cl,OH)$	Light yellow
Kyanite	$Al_2SiO_5(Fe^{3+})$	Colourless
Garnet	$Ca_3Al_2(SiO_4)_3$	Green
Spodumene	$LiAl(Si_2O_6)$	Yellow
Emerald	$Be_3Al_2Si_6O_{18}$	Green
Aquamarine		Light blue
Tourmaline (Elbaite)	$XY_3Z_6(Si_6O_{18})(BO_3)_3(O,OH)_3(OH,F)$	Pink
Quartz Amathyst	SiO_2	Purple

3. Results and discussion

a) Non-silicates

Diamond (Native elements)

As is well known, diamond is the high-pressure, stable polymorph for carbon. Point defects in natural diamond have been studied for at least 30 years [1,13]. Its main impurities, Boron and Nitrogen, are responsible for its luminescence. The main IL diamond emissions previously reported are a blue band (observed in natural and CVD synthetic diamonds), centred at about 430 nm, a 620 nm band related to N-V centres, and a 512 nm band also called "damage peak" for it occurs in diamond after hard irradiation [14,15].

IL emission bands for natural diamond detected in this work is displayed in [Fig. 1]. Our natural diamonds showed emission bands at 412-415 (N_3 centres), 430- 445 (A-band and N-related centres), 502 (H_3 centres) and 637 (N-V centres) nm. However, this characterization should be taken with caution, for research studies over the last 30 years point out that regarding the complexity of the diamond defects, this emission may well come from other kind of imperfections found in its lattice. Further experimental work is therefore needed on this area. Spectra obtained for other diamond samples are very similar.

Our attention was captured by the fact that all the natural diamond samples:

i) independently of their colour, showed a similar IL emission spectrum, suggesting the possibility of characterizing diamond natural samples by their IL spectrum;

ii) the IL emission spectrum presented here is more complex and better defined than those previously reported, indicating the complexity of the traps related to the phenomenon; and

iii) all IL bands detected are related to N-impurities emission centres.

Further studies need to be conducted for more definite results.

Fluorite (Halide)

Fluorite (CaF_2) is present in nature in different colours due to the impurities and defects that it contains. Its structure can
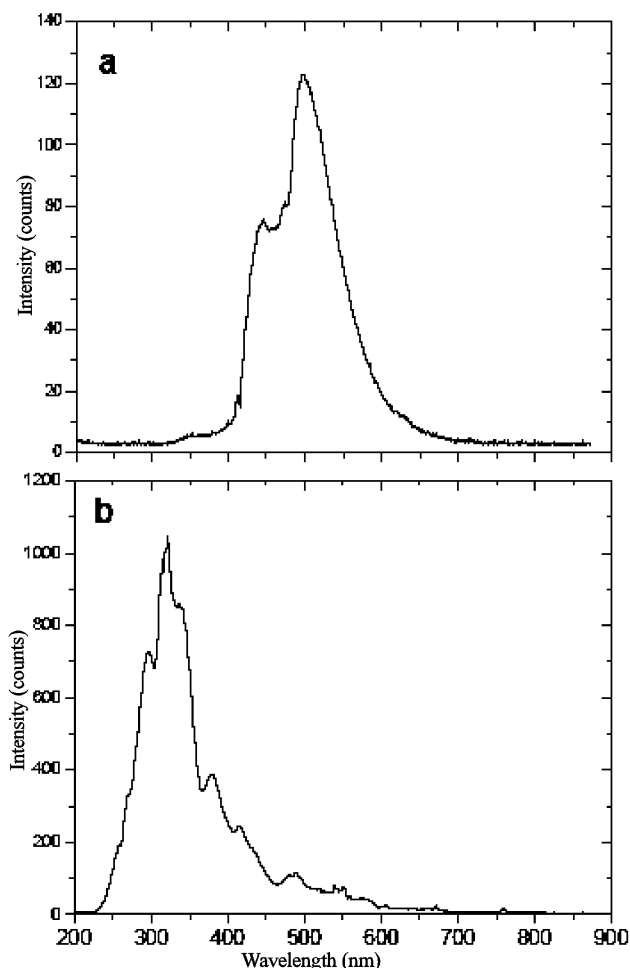
FIGURE 1. IL spectra for non-silicate minerals; (a) Yellow Diamond, (b) Green Fluorite.

be described as an FCC for calcium ions where fluorine ions occupy all the Td positions. Fluorite usually carries impurities such as Y^{3+}, Cs^{2+} substituting Ca^{2+} or rare earths such as Eu^{2+}, Eu^{3+}, Pr^{3+} as well as intrinsic defects.

Figure 1b shows the IL spectrum detected for green fluorite. A broad emission band peaking at 250, 275, 300, 320, 340, 380, 413, and 485 nm, extending from UV, can be observed. The strong UV emissions with maxima near 250, 275, 300 and 420 nm have been detected elsewhere in previous studies [18,19] and attributed to intrinsic defects (F^{3+} an F^+ colour centres) [20]. This latter assumption seems to be supported, in our case, by the fact that these emissions have been also detected in an ultra-pure synthetic fluorite sample studied here.

Ruby and Sapphire (Oxides)

Corundum (Al2O3) is present in nature as two gemstones; ruby (Al_2O_3: Cr^{3+}) and sapphire (Al_2O_3: Fe^{2+}, Ti^{4+}). Colour and luminescence in ruby is due to the presence of chromium while in sapphire, a charge transfer phenomenon between Fe^{2+} and Ti^{4+} is held responsible for both characteristics. Figures 2a, 2b and 2c show the IL spectra for a

natural sapphire, a treated pink one, and a ruby. The expected Cr^{3+} emission at 695nm for the ruby was also detected for both the sapphires. This transition, due to the splitting of the ^2E level, comes along a non-cubic crystal field inside the lattice, and is superimposed on another band that spans from 630 to 750 nm, related to the $^4T_2 \rightarrow ^4A_2$ transition of Cr^{3+}. Emission bands at 330 nm are due to the presence of F^+ colour centres detected in ruby and both sapphires, respectively. F^{3+} centres were observed for the pink sapphire (290 nm).
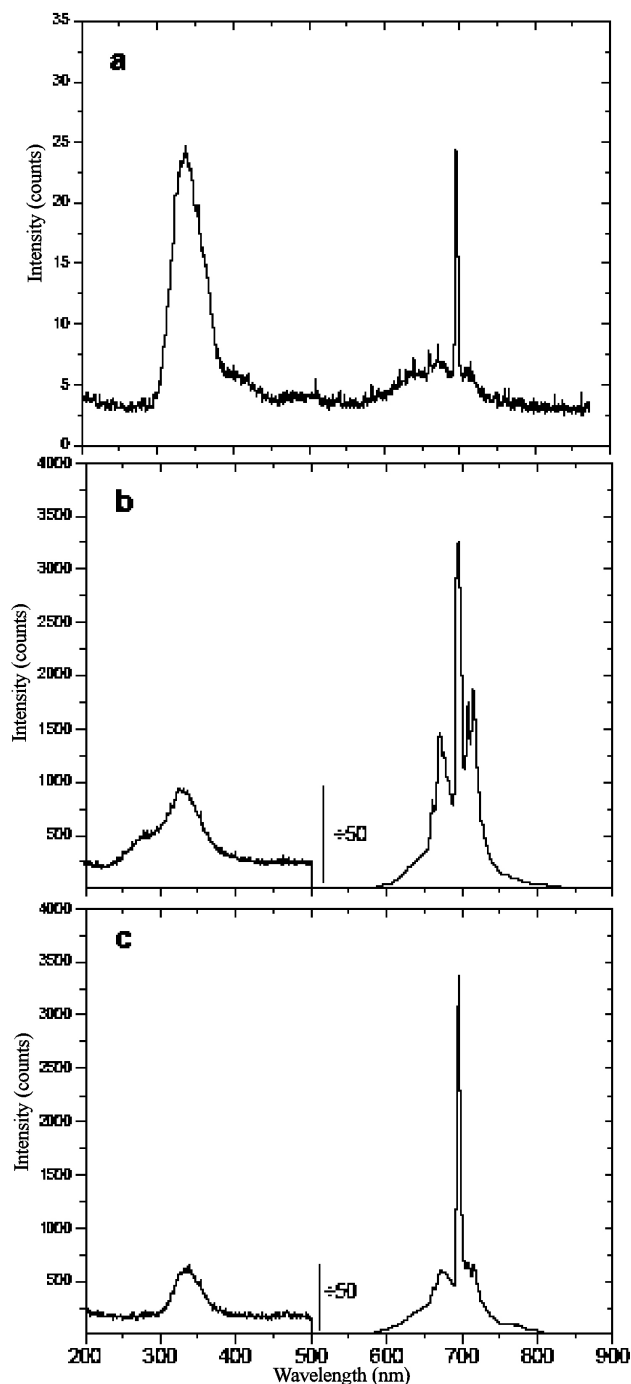

FIGURE 2. IL spectra for non-silicate minerals; (a) Sapphire (b) Treated Pink Sapphire (c) Ruby.
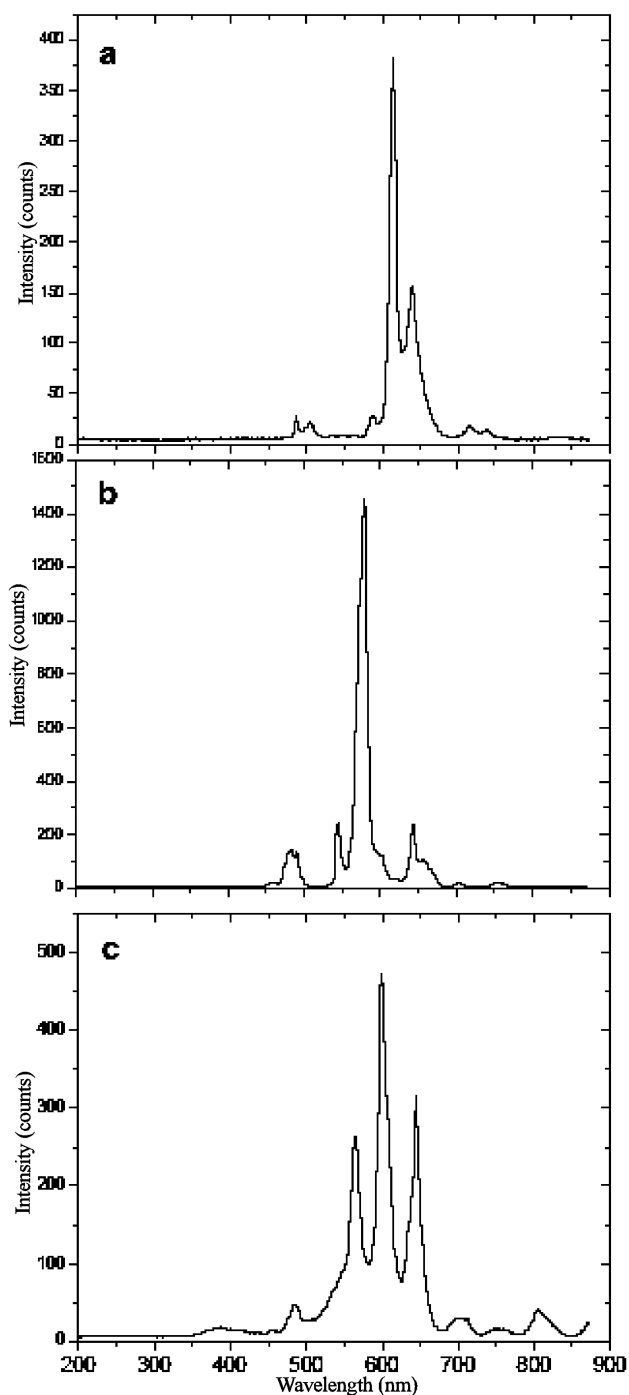
FIGURE 3. IL spectra for non-silicate minerals; (a) Calcite, (b) Strontianite, (c) Apatite.

Calcite and Strontianite (Carbonates) [10]

Ionoluminescence emission representative of calcite ($CaCO_3$) is shown in Fig. 3a. The different bands detected have been previously assigned to different Mn^{2+} transitions, from levels ^4F, ^4D, ^4P, ^4G to level ^6S; the stronger feature is the line near 610 nm assigned to $^4T_{1g} \rightarrow ^6S$ in calcite [11,12]. The overall pattern for orthorhombic carbonates is similar to that observed in rhombohedral ones; Mn^{2+} ions contribute with a red to orange emission, signals varying between line

features and broads bands. Emission spectra for a representative strontianite sample ($SrCO_3$) can be observed in Fig. 3b. Bands detected at 481, 491, 544, 578, 600, 643 and 658 nm can be also related to different transitions of the Mn^{2+} ions. Orthorhombic and rhombohedral carbonates differ in the coordination number of Mn^{2+} ions; while in orthorhombic carbonates Mn^{2+} is surrounded by nine oxygen ions in a distorted polyhedron (Oh symmetry), rhombohedral ones have a six-fold coordination for this ion.

Apatite (Phosphate)

Apatite, ($Ca_5(PO_4)_3(F,Cl,OH)$), belongs to the phosphate group and has an economic interest as a potassium source for fertilizers. It is also a main constituent of bones and teeth. The studied sample is from La Celia mine, in Murcia, Spain. Bands detected at 390, 485, 560, 600, 650, 703, 750 and 810 nm are in good agreement with those previously reported for luminescence studies (excitation-emission) of this mineral. The most intense visible emission, even detectable by the naked-eye, is located in the 500-700 nm spectral range (Fig. 3c). This well-known red emission presents high quantum efficiency and can be attributed to $^1D_2 \rightarrow ^3H_4$ transition Pr^{3+} [16,20].

b) Silicates

Kyanite

Even though Cr^{3+} has sometime been reported to be present in kyanite [21], this mineral tends to have a composition that matches the chemical formula Al_2SiO_5 with apparently only a very limited amount of Fe^{3+} being able to enter the structure. Figure 4a represents its emission spectrum, obtained during the proton beam irradiation. The main feature to be seen is a broad band in near IR wavelength region spectrum from 600 to 800 nm, peaking at 690 nm and 710 nm. These last two bands correspond to the typical emission of Cr^{3+} ions in a nearly cubic intermediate crystal field [22]. The former two, instead, correspond respectively to the so-called R1 and R2 lines associated with the two components of the $^2E \rightarrow ^4A_2$ magnetic dipole transition in a predominantly cubic crystal field; whereas the low energy bands could be due to either to phonon side bands, or R' lines corresponding to Cr^{3+} located in different crystal field sites. The broad band appearing from 600-750 nm is associated with a $^4T_2 \rightarrow ^4A_2$ transition of the Cr^{3+} ion, which happens to be thermally activated at room temperature.

Green Garnet (Grossular)

Although garnet ($R_3^{2+}R_2^{3+}$ $(SiO_4)_2$; $R^{2+}=$ Ca, Mg, Fe, Mn and $R^{3+}=$ Al, Fe, Mn, Cr) is an ideal structure for observing efficient luminescent ions such as Cr^{3+}, Mn^{2+} or Y^{3+}, no sign of those ions has been detected whatsoever in our sample. In fact, the IL emission spectrum of grossular only displays a weak, narrow band located at about 740 nm, that is

related in framework silicates to the $^4T_1 \rightarrow ^6A_1$ ion transition of Fe^{3+} whenever it substitutes Al^{3+} [23-25].

Spodumene

The chemical composition of spodumene does not show any great variation from the ideal formula $LiAlSi_2O_6$; there is no replacement of Si^{4+} by Al^{3+} at all, and only minor substitution of Al^{3+} by Fe^{3+} and Mn^{2+} in M_1 octahedral site occurs. The luminescent spectrum in Fig. 4b can be related to manganese ion Mn^{2+} in octahedral coordination in an M_1 site. The 585 and 620 nm emission bands have been assigned to $^4A_{2g} \rightarrow ^4T_{2g}$ and $^4T_1 g \rightarrow ^6S$ manganese ion transition in distorted octahedral coordination [12,26].

Emerald and Aquamarine

Emerald and aquamarine are the Cr^{3+} and Fe^{3+} respectively rich varieties of beryl; a cyclosilicate with a chemical composition that can be written according to the following expression: $R^+ Be_3R^{3+} R^{2+} Si_6O_{18}$, with R^+ = (Na, K, Cs); R^{2+} would include Fe^{2+}, Mn^{2+} and Mg^{2+} and $R^{3+} = Al^{3+}$, Fe^{3+} or Cr^{3+}. Figure 4c shows the IL spectrum for the emerald sample. Emission bands detected at 690, 715, 735 and 765 nm are very close to those reported for luminescent stud-

ies of Cr^{3+} on this mineral [27]. On the other hand, for the aquamarine sample a very weak signal was observed at 680 nm. This emission is related to the presence of Fe^{3+} [12].

Pink Tourmaline (Elbaite)

Tourmaline is usually considered as: XY_3Z_6 (Si_6O_{18}) $(BO_3)_3$ $(O,OH)_3$ (OH,F) where: $X = Na^+$, Ca^{2+}; $Y = Mg^{2+}$, Fe^{2+}, Mn^{2+}, Li^+, Al^{3+}; $Z = Al^{3+}$, Mg^{2+}, Fe^{3+}. Elbaite is the Al^{3+}, Li^+ member rich of elbaite-chorlo-dravite tourmaline series. Figure 4d shows the IL spectrum of an elbaite tourmaline. Emission lines in the blue (420 nm) and orange (610 nm) range of the spectrum can be related to $^4G \rightarrow ^6S$ of the Mn^{2+} ion transition (590 and 620 nm). Manganese should be located in octahedral Y sites, surrounded by oxygen and (OH-) ions. Similar results were reported for tourmalines in Ref. 13.

Quartz–Amethyst

Quartz (SiO_2) is probably one of most studied minerals in luminescence. Thermoluminiscence archaeological dating, dose determination, optically stimulated luminescence dating, and diverse defect characterization have been applied to it. Luminescent studies reveal the complexity of its emission
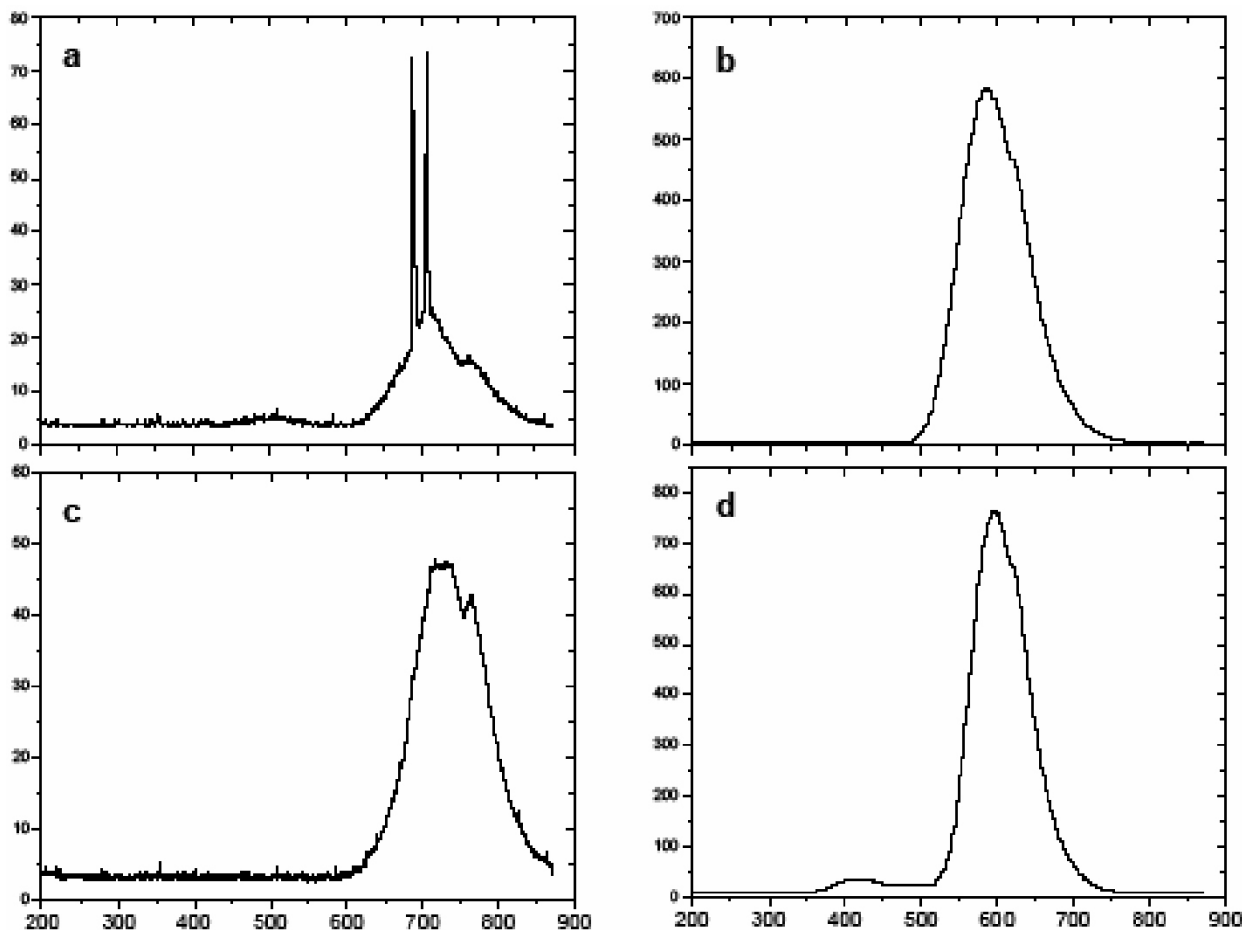

FIGURE 4. IL spectra for silicate minerals; (a) Kyanite, (b) Spodumene, (c) Emerald, (d) Pink Tourmaline.
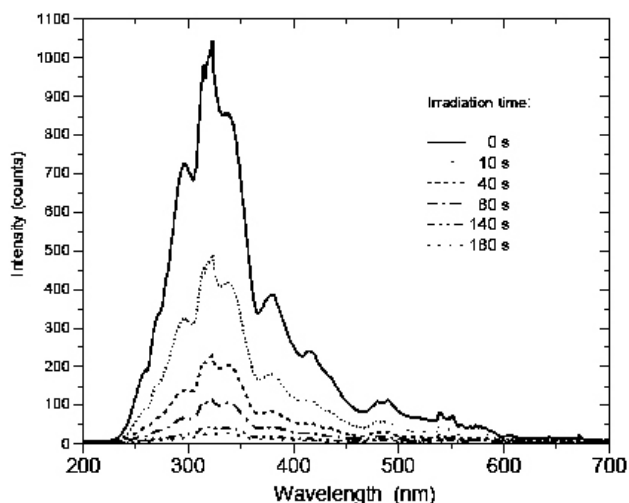
FIGURE 5. IL spectra for green Fluorite as a function of the irradiation time from 0 to 180 s. Proton beam current on the sample was 150 nA.

mechanisms and the diversity of traps responsible or related to them. Weak signals at 560 and 650 nm have been detected. These emissions have been reported as C and D bands [28], related to wet-grown SiO_2 defects, and, to some extent, to (OH-) and H_2O molecular groups. Luminescent data for quartz are known to be complex and the interpretation of the mechanisms responsible for emission and defect assignation are still open questions.

c) IL emission spectrum variation with time

Light intensity variation as a function of time was observed for all samples studied. For instance, the green fluorite's homogeneous decreasing emission with time can be seen in Fig. 5 from 0 to 180 s. Proton beam current on the sample was 150 nA. IL intensity variations with time have been previously reported and related to different effects such as sample heating or amorphousization [8,13]. Other studies that mention the increase in the sample's temperature that accompany its proton irradiation explain this phenomenon by taking into account an excitation-spike model [29].

In general, all IL data presented in this work are very similar to other reported data, mainly in photoluminescence studies. This seems to suggest that, to some degree, the mechanism responsible for the emissions detected is similar for both cases, notwithstanding the fact that in an IL measurement, there is usually an amorphousization process also taking place [13,29]. We suggest that in order to understand IL process emission, the Excitation-Spike Model [30] which includes:

(i) excitation of the electronic system,

(ii) slowing down of the electron and phonon creation (heating),

(iii) location of the energy as trapped (self- trapped or trapped at a defect centre) excitons and

(iv) non radiative decay of the excitons; needs to be considered together with a radiative emission model.

Our data suggest that both mechanisms (non-radiative and radiative transitions) compete during the proton-irradiation process. The increase in temperature (amorphousization) implies a decrease in the radiative transition and an increase in non-radiative emissions.

4. Conclusions

Emission spectra during proton irradiation (IL) have been obtained for a set of minerals of historical/artistic interest. Main conclusions are:

i) Cr^{3+} ion has been detected for some minerals; sapphire, kyanite and emerald. chromium in sapphire and kyanite is present in very low concentration, therefore IL proves to be an extremely sensitive method for detecting this impurity.

ii) Mn^{2+} ions have been detected for calcite, spodumene, and Fe^{3+} for Aquamarine.

iii) Pr^{3+} ion has been detected for apatite crystals.

iv) A set of intrinsic defects, as well as those irradiation induced, namely in sapphire, fluorite and diamond, have been also detected.

A reduction in luminescence emission as a function of the time was observed for most of the minerals. Mechanisms of non-radiative and radiative transitions compete during the proton-irradiation but when the temperature increases, the amorphousization process favours the non-radiative emissions. IL spectroscopy is a very useful method fot understanding material phenomena such as

i) radiation-matter interaction,

ii) impurity characterization;

iii) local symmetry studies,

iv) origin, colour and provenance studies of minerals.

The data presented give a general overview of the technique's potential for the identification of minerals and contribute to the creation of a new IL database that will be of much use for future applications. We truly believe that IL has an important role to play not only as an analytical tool in the mineralogical and archaeometric field, but also in radiation-matter interaction studies.

Acknowledgements

1. T. Calderón, A. Millán, F. Jaque, and J. García-Solé, *Nucl. Tracks Radiat. Meas. 17* (1990) 557.

2. H.M. Rendell, M.R. Khanlary, P.D. Townsend, T. Calderón, and B.J. Luff, *Mineral Magazine 57* (1993) 217.

3. Gunnell and E. Mitchell, *America Mineralogist 18* (1993) 68.

4. H. Rendell, T. Calderón, A. Pérez-González, J. Gallardo, A. Millán, and P.D. Townsend, *Quaternary Geocronology* **13** (1994) 429.

5. A.G. Wintle, *Radiation Protection Dosimetry* **47** (1993) 627.

6. M.J. Aitken, *Science-based Dating in Archaeology* (Longman, London, 1990).

7. Y. Sha, P. Zhang, G. Wang, X. Zhang, and X. Wang, *Nucl. Instr. & Meth. B* **189** (2002) 408.

8. C. Yang, K.G. Malmqvist, M. Elfman, P. Kristiansson, J. Palon, A. Sjöland, and R.J. Utui, *Nucl. Instr. & Meth. B* **130** (1997) 746.

9. O. Enguita *et al.*, *Nucl. Instr. & Meth. B* **219/220** (2004) 53.

10. H. Calvo del Castillo *et al.*, *Nucl. Instr. & Meth. B* **249,1/2** (2006) 217.

11. H. Calvo del Castillo, J.L. Ruvalcaba, and T. Calderón, *Anal. Bioanal. Chem.* **387** (2007) 869.

12. T. Calderón *et al.*, *Radiat. Meas.* **26** (1996) 719.

13. T. Calderón and R. Coy-Yull, *Journ. Gemmology, XVIII (3)* (1982) 217.

14. H.M. Rendell, M.R. Kahanlary, P.D. Townsend, T. Calderón, and B.J. Luff, *Mineral Magazine* **57** (1993) 217.

15. T. Calderón, M.R. Khanlary, H.M. Rendell, and P.D. Townsend, *Nucl. Tracks Rad. Meas.* **20** (1992) 475.

16. E. Cantelar *et al.*, *Jour. Alloy & Compounds* **323/324** (2001) 851.

17. A.M. Zaitsev, *Optical properties of Diamond* (Springer, Berlin, 2001).

18. C.M. Subramanian and M.L. Mukherjee, *J. Mater. Sci.* **22** (1987) 473.

19. S.A. Holgate, T.H. Sloane, P.D. Townsend, P.D. White, and A.V. Chadwick, *J. Phys. Condens. Matter* **6** (1994) 9255.

20. V.A. Skuratov, S.M. Abu Al Azm, and V.A. Altynov, *Nucl. Instr. & Meth. B* **191** (2002) 251.

21. W. Deer, R.A. Howie, and J. Zussman, *The Rock Forming Minerals* (Prentice Hall, London, 1992).

22. A.N. Tarashchan, *Luminescence of minerals* (Naukova Dumka, Kiev, 1978).

23. J.E. Geake and G. Walker, *Infrared and Raman spectroscopy of lunar and terrestrial minerals* (Academic Press, New York, 1975) p. 73.

24. W.B. White, M. Masako, D.G. Linneham, T. Furukawa, and B.K. Chandrasekahr, *Am. Mineral* **71** (1986) 1415.

25. A.A. Finch and J. Klein, *Contrib. Mineral Petrol.* **135** (1999) 234.

26. A.S. Marfunin, *Spectroscopy, Luminsecence and Radiation Centers in Minerals* (Springer, Berlin, 1979) p.196.

27. E.M. Flangen, D.W. Breck, N.R. Mumbach, and A.M. Taylor, *Am. Mineral.* **52** (1967) 744.

28. H. Koyama, *J. Appl. Phys.* **51** (1980) 2228.

29. N. Itoh and A.M. Stoneham, *Nucl. Instr. & Meth. B* **146** (1998) 362.

30. G.H. Dieke, *Spectra and Energy of Rare Earth Ions in Crystals* (Wiley Interscience, New York, 1988).